Chapter 6

Factors affecting ocular dominance stripe formation

6.1 Introduction

This chapter considers the mechanisms driving the development of ocular dominance stripes in some of the main models reviewed in Chapter 3. The first half of the chapter considers why stripes, rather than segregated layers, are formed in these models. Simulations of the model by Obermayer et al. (1991) are replicated, which show how ocularity variance controls stripe width in a two-dimensional postsynaptic sheet. In the second half of this chapter, the Obermayer model is extended with a three-dimensional postsynaptic block to see how topography and ocularity map into a three-dimensional output space representing the LGN.

6.2 Reasons for ocular dominance stripe formation in models

Most of the models of ocular dominance reviewed in Chapter 3 form stripes of alternating eye input rather than completely segregated regions for each eye. This is in contrast to the model investigated in this thesis which generates completely segregated eye-specific regions. There are three different arguments for why stripes form in models:

1. Lateral interactions
2. Competition between topography and ocularity
3. Primary/secondary feature argument

Each of these arguments are now considered in turn.

6.2.1 Lateral interactions

Some models of ocular dominance do not consider the development of topography (Swindale, 1980; Miller et al., 1989). In these models, the major determiner of stripe width is the extent of the lateral interactions amongst postsynaptic units. The local excitatory connections encourage nearby pairs of units to be correlated, and therefore adapt to similar stimuli. The longer-range inhibitory connections perform the opposite task of ensuring that pairs of distant units are anticorrelated, preventing them from adapting in the same direction to the input stimuli. Miller's model is slightly more complicated: in the absence of inhibitory lateral connections, as long as there is presynaptic normalisation then stripes still develop (Miller et al., 1989).

6.2.2 Competition between topography and ocularity

For those models considering the development of both ocular dominance and topography, stripes arise through competition between these two features as well as the extent of the lateral interactions (von der Malsburg, 1979; Goodhill, 1992; Andrade & Moràn, 1996). Neighbouring presynaptic units from the same eye ("same-eye units") tend to connect to the same region of the postsynaptic sheet. Similarly, units at the same retinotopic position but from different eyes ("same-position units") tend to connect to the same postsynaptic region. If these two tendencies are roughly equal, a compromise is made whereby neighbouring postsynaptic units receive inputs from either units from the same eye but different positions, or from the same position but different eyes. Stripes form as a consequence of these two competing tendencies.

What are the mechanisms underlying the tendency for presynaptic units to connect to the same region of the postsynaptic sheet? The correlated activity of same-eye units ensures that they connect to similar parts of the postsynaptic sheet. For same-position units however, there are two different mechanisms at work. First, if there are positive between-eye correlations, pairs of same-position units are likely to be positively correlated. This correlated activity will ensure that they connect to the same region of the postsynaptic sheet. Second, the initial weights of the network are usually biased so that same-position units initially connect to roughly the same region of the postsynaptic sheet. So, even in the absence of any positive between-eye correlations, same-position units will connect to similar regions of the postsynaptic sheet as long as the initial weights are appropriately biased. (This is seen for example in Goodhill's model (Goodhill, 1992, p90) when the correlation parameter $h = 0$ which produced no between-eye correlations.)

Under this framework, stripe width is affected by the relative strengths of the correlations of same-eye units and same-position units. When pairs of same-eye units are more correlated than same-position units, the stripes tend to be quite wide — many neighbouring postsynaptic units respond to the same eye. As the strength of the same-position correlations increase relative to the same-eye correlations, stripe width decreases as some neighbouring postsynaptic units tend to connect to same-position units in preference to same-eye units.

6.2.3 Primary/secondary feature argument

The work by Obermayer et al. (1991) put a different perspective on why stripes arise and the mechanisms controlling stripe width. They considered a five-dimensional feature vector, (x, y, ϕ, q, z), to represent a pattern of activity distributed across two retina. Features x and y represented the centre of mass of the stimuli, ϕ and q the orientation of the stimuli, and z the ocularity of the stimuli. Feature vectors were input to a Kohonen network with a two-dimensional arrangement of postsynaptic units. In this model, the Kohonen network was required to perform dimension reduction: to map from a five-dimensional input space to a two-dimensional output space. This had previously been investigated as an abstract mapping problem (Kohonen, 1988; Ritter & Schulten, 1988). In such situations, the network automatically discovers the elements of the input vector with highest variance, and represents them in the network. Other elements of the input vector with variance below a critical value do not get represented in the map (Ritter & Schulten, 1988). This is referred to as the "automatic selection of feature dimensions" (Kohonen, 1988). As is shown in more detail in the next section, the variance of the ocularity feature controls stripe formation: the higher the ocularity variance (compared with the other input variances), the wider the ocular dominance stripes.

6.3 Obermayer's model for stripe formation

All of the models mentioned in the last section provide different reasons for how stripe width varies under different conditions. Out of all of the models, the model by Obermayer et al. (1991) is arguably the simplest because it uses feature vectors to represent the neural activity distributed across two retinae. This model has therefore been chosen to investigate the nature of stripe formation in the cortical simulations. We also extend the postsynaptic sheet into a three-dimensional block so that the model can be applied to the problem of retinogeniculate development.

6.3.1 Implementation details of Obermayer experiments

The network consists of a presynaptic sheet with three units fully connected to a set of postsynaptic units. The postsynaptic units are arranged into a three-dimensional block for the purposes of neighbourhood weight updating. (For the two-dimensional simulations, the Z dimension of the postsynaptic block was set to one.)

The initial weights are set at random, with no topographic or ocular bias. One iteration of the model consists of generating and presenting a feature vector, calculating postsynaptic unit activations and updating the weights of the winning and neighbouring units. One epoch of the model corresponds to 100 iterations, after which various parameters, such as the weight-update rate and size of neighbourhood, are updated. Table 6.1 describes the equations and parameters used for these experiments.

6.3.2 Visualisation of maps formed in Obermayer experiments

Each postsynaptic unit receives inputs via three weights. The first two weights code for the centre of mass and the third weight codes for the ocularity to which the unit is most responsive. Visualisation of each postsynaptic unit's preferred stimulus is straightforward. The centre of mass for each postsynaptic unit j is drawn on a graph at the point ($x = w_{1j}$, $y = w_{2j}$). Lines are drawn between the points of neighbouring postsynaptic units to indicate the location of neighbouring postsynaptic units. The ocularity of each postsynaptic unit is encoded in $z = w_{3j}$. The value of z for all postsynaptic units is visualised using a Hinton diagram — the size of the square is proportional to the magnitude of z (scaled to a maximum size of z_{pat}) and the colour of the square indicates the sign of z (black for negative values representing dominant left-eye input and white for positive values representing dominant right-eye input).

6.3.3 How the variance of ocularity affects stripe width

To illustrate the principle of feature selection within the standard cortical model, several experiments similar to those presented in (Obermayer et al., 1991) were replicated. Three-dimensional

Inputs	$x_1 = \text{rnd}(0,15), x_2 = \text{rnd}(0,15), x_3 = \pm z_{pat}$
Activation rule	$y_j = \sum_{i=1}^{3}(w_{ij} - x_i)^2$
Winner	Find m: $\quad y_m \leq y_j \ \forall j$
Weight modification	$\Delta w_{ij} = \varepsilon(t)d(j,m)(x_i - w_{ij})$ $\qquad$ (t is the epoch number)
Distance measure	$d(j,m) = n(P_x(m) - P_x(j), P_y(m) - P_y(j), P_z(m) - P_z(j))$
Index function	$j = P_x(j) + (X_{\text{post}} \times P_y(j)) + ((X_{\text{post}} \times Y_{\text{post}}) \times P_z(j))\dagger$
Neighbourhood function	$n(x,y,z) = \exp(\frac{x^2}{\sigma_x^2} + \frac{y^2}{\sigma_y^2} + \frac{z^2}{\sigma_z^2}), \qquad \lvert x\rvert \leq r_x, \lvert y\rvert \leq r_y, \lvert z\rvert \leq r_z$
Rate of weight-update	$\varepsilon(t) = \begin{cases} 0.05 & t \geq 1000 \\ \min(0.05, \varepsilon_0 - \text{floor}(t/50) \times 0.1) & \text{otherwise} \end{cases}$

† Given the index j for a postsynaptic unit, its position within the three-dimensional postsynaptic block, $(P_x(j), P_y(j), P_z(j))$, can be calculated using this equation.

Parameter	Value
Number of epochs	1000
Initial weight-update rate, ε_0	0.8
Inputs per epoch	100
Postsynaptic block size (X_{post},Y_{post},Z_{post})	(32,32,Z)

Epoch	(r_x, r_y, r_z)	$(\sigma_x, \sigma_y, \sigma_z)$
0	(5,5,5)	(3.0, 3.0, 3.0)
200	(3,3,3)	(2.0, 2.0, 2.0)
500	(1,1,1)	(1.0, 1.0, 1.0)

Table 6.1: Network equations and parameters used for Obermayer experiments. The only parameters varied in the experiments presented in this chapter were Z, which controlled the size of the postsynaptic block, and z_{pat}, which determined the degree of ocularity variance in the input vector. Network equations are the same as those used by Obermayer et al. (1991).

input vectors (x, y, z) were used as input to a Kohonen network with a two-dimensional sheet of postsynaptic units of size $X_{\text{post}} = 32, Y_{\text{post}} = 32$ (assuming $Z_{\text{post}} = 1$). Each feature vector represented a pattern of activation across two notional retinas. The features x and y coded for the centre of mass of the activation, whereas z encoded the degree of monocularity of the activation over the two notional retinas. The higher the value of z, the more monocular the input stimuli. Rather than presenting patterns of activity on two retinas and then calculating the feature vector, the feature vectors were directly generated. The x and y elements were independently chosen at random from the uniform distribution $[0, 15]$ and z was set to $\pm z_{pat}$, with the sign of z chosen at random. z_{pat} was a control parameter which was varied in experiments.

Figure 6.1 shows the effect of varying the z_{pat} parameter on map development. Table 6.2 shows the number of postsynaptic units responsive to each eye along with the mean ocularity strength. When z_{pat} is small, the ocularity component of the input vector is largely ignored, and the map smoothly represents the x, y parameters (Figure 6.1(a)). In this map, visual space is regarded as a primary feature because the map is ordered according to the values of (x, y). As z_{pat} increases above its first critical threshold ($z_{pat} = 0.6$), the network has to code for all three features of the input vector, producing the slightly bumpy map of visual space. Thin stripes are present in the map's representation of the z parameter (Figure 6.1(b)), but visual space is still the primary map feature. In this map, ocularity is a secondary feature because the map represents the same value of z in more than one region of the postsynaptic sheet. As z_{pat} is further increased, the map of visual space becomes more convoluted as it has to account for the wider ocularity stripes (Figure 6.1(c)).

Once z_{pat} exceeds a second critical value ($z_{pat} = 2.0$), ocularity becomes the primary map feature and visual space is relegated to a secondary feature (Figure 6.2). In this network, each point of visual space is represented twice in the postsynaptic sheet, once for each eye. The map of visual space has folded over on itself, which is more clearly seen in Figure 6.2(b) when the topographic map is plotted separately for postsynaptic units with positive and negative values of z.

The feature vector representation used here is much more abstract than an explicit representation of neural activity in two retina as used in other models. However, in agreement with the other models, it also predicts that the more monocular the stimuli, the wider the strips. (Due to the way the feature vectors were generated, it is difficult to directly interpret z in terms of between-eye correlations. A simple approximation is that when $z = 0$, the two eyes are completely correlated, and as z increases, the between-eye correlations decreases.) The model also shows, however, that if the variance of the ocularity is sufficiently high, the ocular map segregates into two eye-specific regions.

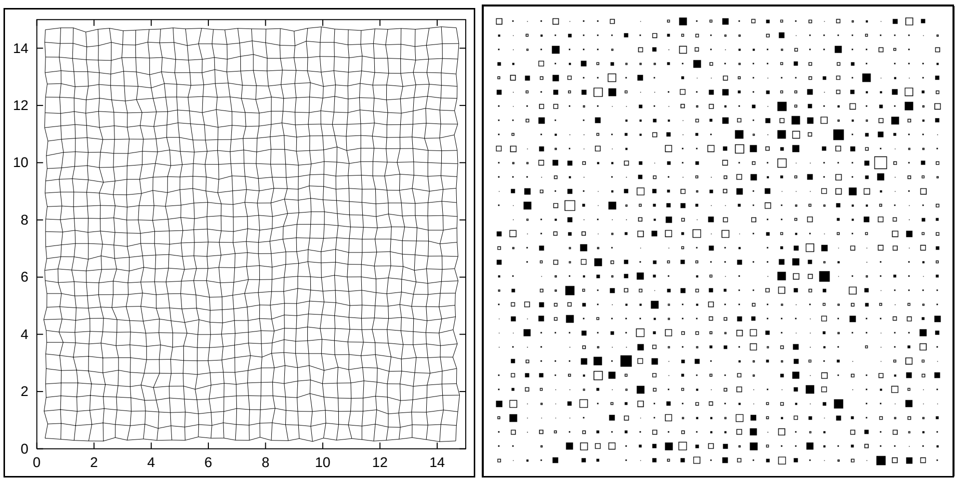

(a) $z_{pat} = 0.2$

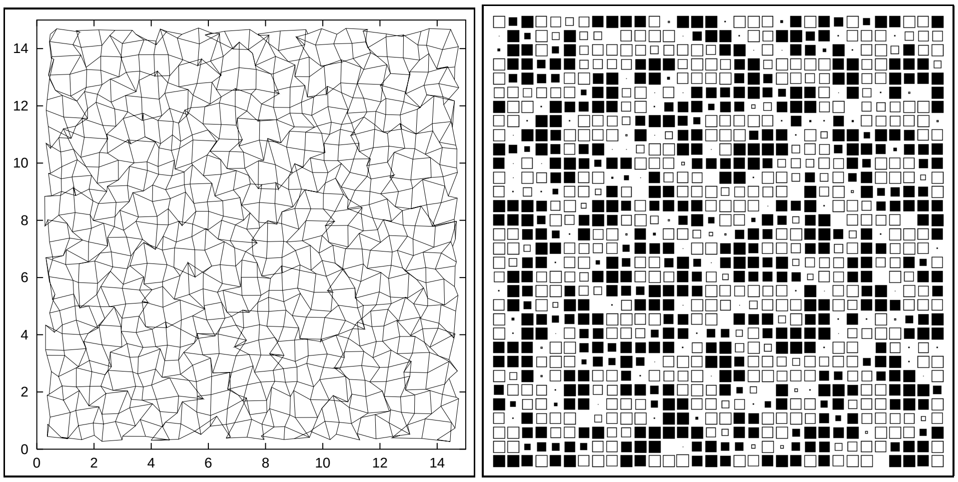

(b) $z_{pat} = 0.6$

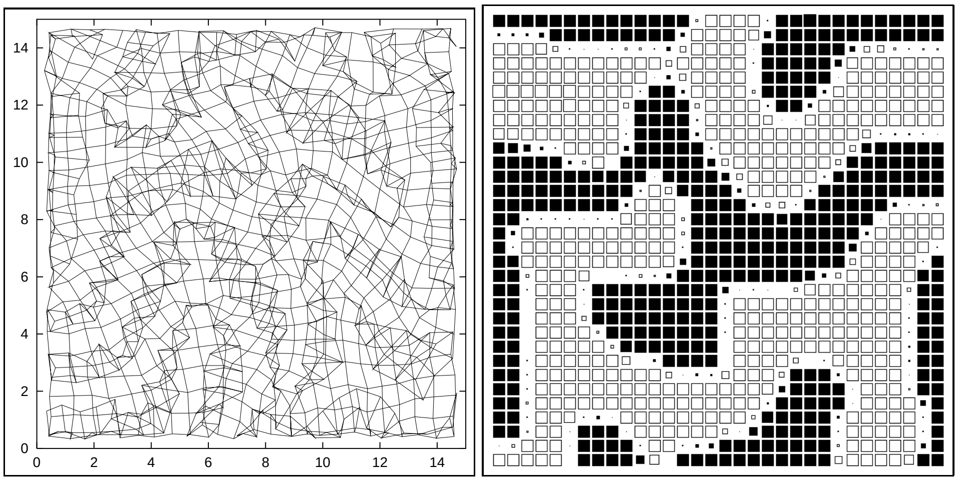

(c) $z_{pat} = 1.0$

Figure 6.1: Final topography and ocularity maps in a two-dimensional Kohonen network with feature vectors $(x, y, \pm z_{pat})$ as input and $z_{pat} = 0.2, 0.6, 1.0$. (a): $z_{pat} = 0.2$. (b) $z_{pat} = 0.6$. (c) $z_{pat} = 1.0$. See also Table 6.2 for mean z values.

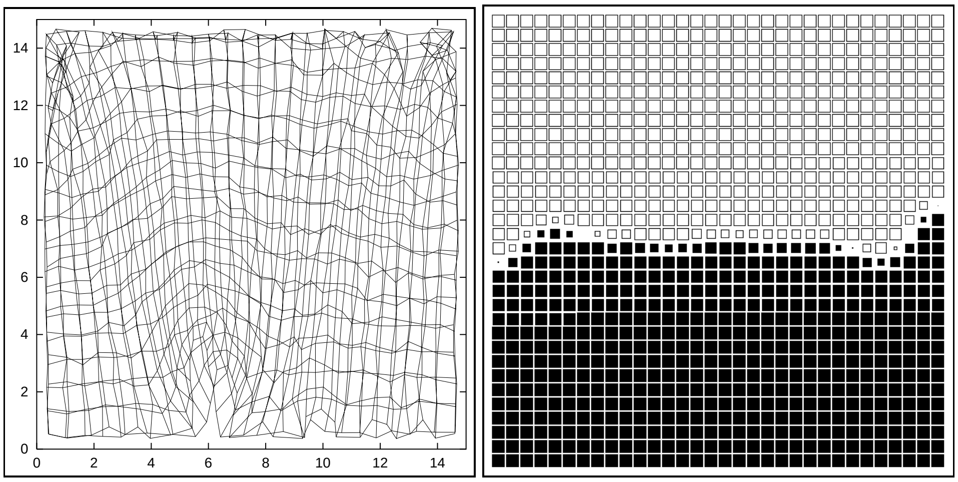

(a) Topography and ocularity plots ($z_{pat} = 2.0$)

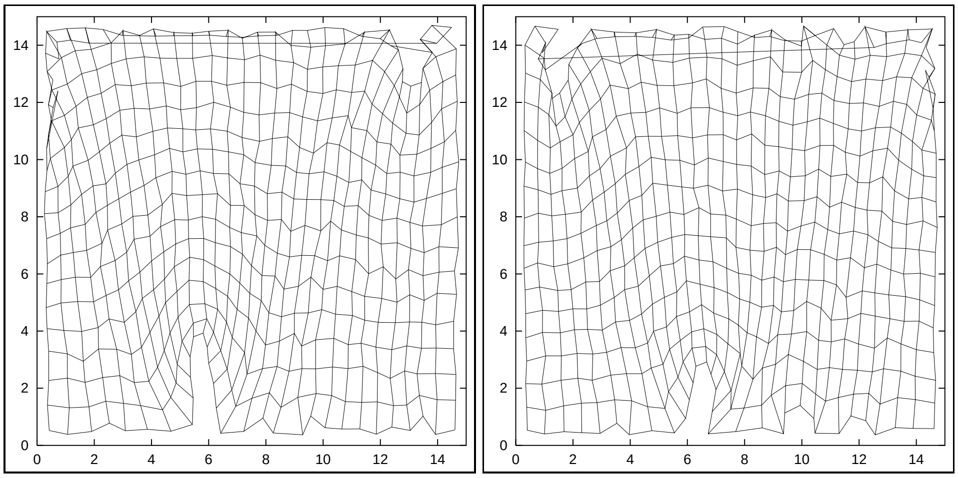

(b) Representation of visual space for each eye ($z_{pat} = 2.0$)

Figure 6.2: Final topography and ocularity maps in a two-dimensional Kohonen network with feature vectors $(x, y, \pm z_{pat})$ as input and $z_{pat} = 2.0$. (a): Topography and ocularity plots. Conventions for plots same as in Figure 6.1. (b): Topography plots for each eye. In the left (right) plot, the (x, y) values from weight vectors are plotted for units with a negative (positive) z value. Lines are drawn between the points representing nearest vertical and horizontal units with the same sign of z. The 32×32 postsynaptic sheet has divided into two maps of size 32×16 representing visual space independently for each eye. The kinks at the bottom of each map (above the point $x = 6$) arise from a rectangular map (of width 32 and height 16 units) uniformly covering a square input space.

6.4 A new model of retinotopic map formation in the LGN

In the previous experiments, the units in the postsynaptic sheet were arranged in a two-dimensional sheet. In the experiments presented in this section, the postsynaptic sheet is extended into a three-dimensional block to make the model similar to the LGN. The three-dimensional arrangement of the postsynaptic block is shown in Figure 6.3. All other elements of the model remained the same.

When the network is presented with the three-dimensional feature vector, postsynaptic units become monocular even with values of z_{pat} that were too low for ocularity to be represented in the two-dimensional network. Figure 6.4 shows the results of presenting the same retinal inputs as used in the two-dimensional experiments into the three-dimensional postsynaptic block of size ($X_{\text{post}} = 32, Y_{\text{post}} = 32, Z_{\text{post}} = 4$), for $z_{pat} = 0.2$ and $z_{pat} = 2.0$.

To analyse the maps, the three-dimensional postsynaptic block has been divided into multiple two-dimensional planes (as illustrated in Figure 6.3). Z-plane n corresponds to all of the units in the plane $Z = n$ of the postsynaptic block. Figure 6.4 shows the results of network development with $z_{pat} = 0.2$. In this case, the top two Z-planes of the network responded to the right eye and the bottom two Z-planes of the network to the left eye. Within each Z-plane, the representation of visual space was complete and topographic. Figure 6.5 shows the topographic maps from the same network when the postsynaptic sheet is divided into multiple X-planes. (X-plane n corresponds to all of the units in the plane $X = n$ of the postsynaptic block.) Each X-plane covers a small part of the visual space, but all of the X-planes taken together cover the entire visual space. Additionally, neighbouring X-planes cover neighbouring parts of the visual space. (X-planes 1 and 32 cover a slightly larger region of visual space than the other planes due to boundary effects.) The X-planes are similar to the projection columns found in the LGN (Sanderson, 1971a).

However, with a bigger value of z_{pat}, such as $z_{pat} = 2.0$, ocularity is the primary map feature and visual space a secondary feature (similar to the two-dimensional network shown in Figure 6.2). Each Z-plane of the network developed in the same manner, although the border between left- and right-eye regions varied systematically through the planes. In Figure 6.4, the left half of each Z-plane is responsive to the right eye, and the right half of each Z-plane is responsive to the left eye. In this case, the topographic plots in both the X- and Y-planes show no correspondence with the LGN projection columns. A sample of some topographic maps in the X- and Y-planes are shown in Figure 6.6. For the X-plane plots we find that the maps for the planes equidistant from the centre (X-planes i and $33 - i$ for all values of $i = 1 \ldots 16$) cover almost the same region of the input space. For each pair of X-planes, X-plane i contains units responsive to the right eye, and X-plane $33 - i$ contains units responsive to the left eye. In contrast, each Y-plane topographic plot has folded over on top of itself, so that each part of visual space is covered by two units (one for each eye) in each Y-plane.

6.5 Correspondence with topography and ocularity in the LGN

The cat LGN has a very distinctive three-dimensional shape, as shown in Figure 2.3. It can be approximated however as a three-dimensional block of postsynaptic units, with roughly equal extent in the lateral-medial (X) and anterior-posterior (Y) dimensions, but a much smaller dorsal-ventral (Z) extent. The maps in Figure 6.4 can be compared with the retinotopic and ocularity

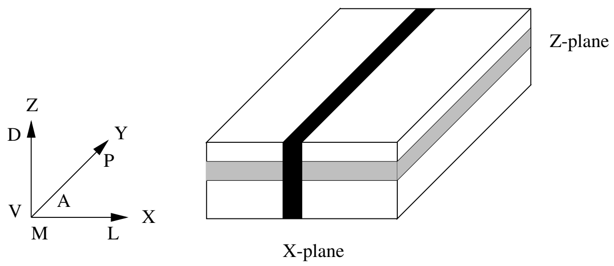

Figure 6.3: Three-dimensional arrangement of postsynaptic units in the Kohonen network. Postsynaptic units are positioned uniformly throughout the three-dimensional block. The X dimension of this block corresponds to the medial—lateral dimension of the LGN. Likewise, the Y dimension corresponds to the anterior—posterior dimension, and the Z dimension corresponds to the dorsal—ventral dimension. The figure shows two different two-dimensional slices through the postsynaptic block. The grey slice is a Z-plane which samples all postsynaptic units at the same dorso-ventral position. The black slice is a X-plane which samples all postsynaptic units at the same medio-lateral position. Key: A – anterior. P – posterior. D – dorsal. V – ventral. L – lateral. M – medial.

mappings within the LGN.

First, when $z_{pat} = 0.2$, the plots show a similar retinotopic organisation to that found in the LGN: units at the same (X,Y) position but at different depths (Z) receive input from the same part of visual space. Furthermore, the map has segregated into eye-specific layers (where a layer is used here to mean the same as a Z-plane) in the same way as the LGN. (In the LGN, the contralateral inputs always innervate the top of the LGN. In these experiments there is no preference for the contralateral inputs to go to the top of the LGN, and so the eye providing input to the top Z-plane varies from simulation to simulation. It should be relatively simple to ensure that the contralateral eye always dominates the top half of the postsynaptic block by placing a suitable bias on the initial weights.) The map has automatically oriented itself to represent the input features with the highest variance (x,y) along the largest dimensions of the postsynaptic block (X,Y). The remaining input feature with the smallest variance, z, is mapped onto the smallest dimension of the postsynaptic block (Z).

This segregation into eye-specific layers is dependent however on the number of Z-planes in the postsynaptic block. When $Z = 4$, the network can easily divide into two halves, so that Z-planes 1 and 2 can respond to one eye, and Z-planes 3 and 4 can respond to the other eye. When $Z = 3$ however, the network fails to completely segregate into separate layers, as shown in Figure 6.7. Monocular units for each eye are found in each Z-plane, although as shown in Table 6.2, there is a tendency for units from the left eye to settle in Z-planes 1 and 2 and for the right eye to settle in Z-planes 2 and 3. This non-complete segregation into eye-specific layers also affects the topography of units within each layer: units responding to different eyes respond to different parts of the visual space. This failure to segregate into eye-specific layers is most likely to be due to the odd number of Z-planes in the network, making it impossible for an equal number of Z-planes to be responsive to each eye.

However, when $z_{pat} = 2.0$, the map develops a different retinotopic and ocular structure to that found in the LGN. For the map in Figure 6.4, the primary feature, ocularity, is mapped along the X dimension of the postsynaptic block, rather than the Z dimension as before. The remaining inputs, (x and y), map along the X and Y dimensions of the postsynaptic block. The structure of the map within each Z-plane is almost identical, except for a shift in boundary position between different ocularity values. This does not correspond to the topographic and ocularity maps found in the LGN, since both space and ocularity are primary features in the LGN.

				$z > 0$ (right eye)		$z < 0$ (left eye)	
Figure	z_{pat}	Z_{post}	Z-plane	n	mean ± s.d.	n	mean ± s.d.
6.1(a)	0.2	1	1	529	0.039 ± 0.029	495	-0.041 ± 0.030
6.1(b)	0.6	1	1	503	0.475 ± 0.162	521	-0.474 ± 0.154
6.1(c)	1.0	1	1	545	0.854 ± 0.301	479	-0.851 ± 0.305
6.2	2.0	1	1	509	1.964 ± 0.177	515	-1.962 ± 0.191
6.7	1.0	3	1	310	0.741 ± 0.306	714	-0.877 ± 0.230
			2	523	0.673 ± 0.347	501	-0.671 ± 0.346
			3	731	0.880 ± 0.227	293	-0.770 ± 0.305
6.4	0.2	4	1	1016	0.180 ± 0.028	8	-0.044 ± 0.026
			2	967	0.122 ± 0.034	57	-0.086 ± 0.041
			3	72	0.094 ± 0.035	952	-0.122 ± 0.032
			4	24	0.040 ± 0.037	1000	-0.178 ± 0.033
6.4	2.0	4	1	554	1.938 ± 0.284	470	-1.893 ± 0.383
			2	541	1.891 ± 0.351	483	-1.937 ± 0.216
			3	479	1.930 ± 0.244	545	-1.890 ± 0.355
			4	468	1.885 ± 0.390	556	-1.947 ± 0.242

Table 6.2: Mean values of z for the two- and three-dimensional Obermayer experiments. The number of units with values of z greater than (right eye) and less than (left eye) zero are shown for each experiment, along with the mean and standard deviation of z. The left-hand column indicates the figure number where the relevant maps are displayed.

$z_{pat} = 0.2$ $z_{pat} = 2.0$

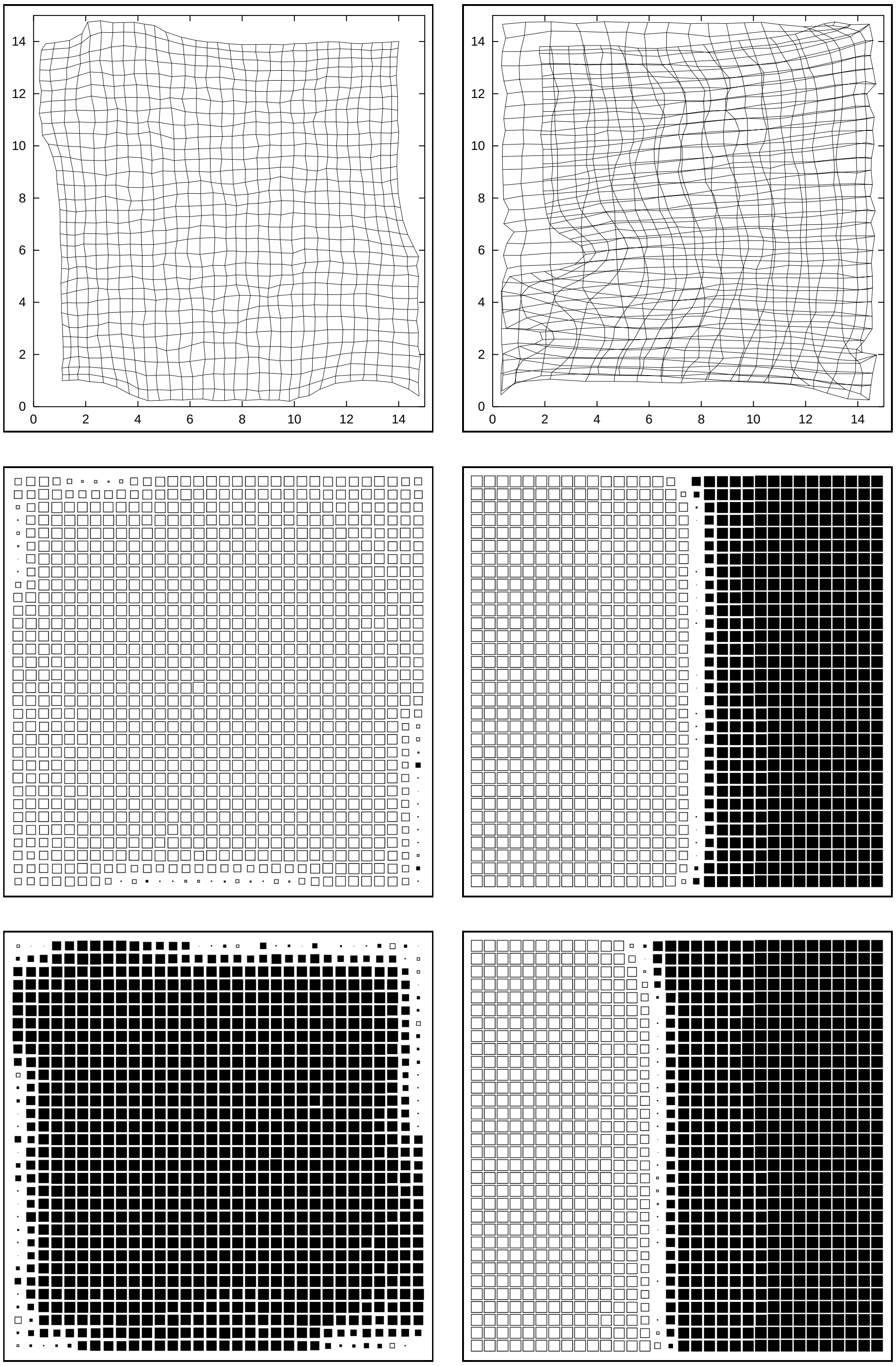

Z-plane 1

Z-plane 1

Z-plane 4

Figure 6.4: Final topography and ocularity plots for three-dimensional feature vector (x, y, z) mapping into a three-dimensional postsynaptic block for $z_{pat} = 0.2$ and 2.0. The top row shows the topography plots for all of the units in the top Z-plane ($Z = 1$) of the postsynaptic block. The maps for the other Z-planes are similar and so are not shown. The middle and bottom rows show the ocularity plots for units in the top ($Z = 1$) and bottom Z-planes ($Z = 4$) of the network. For $z_{pat} = 0.2$, Z-planes 1 and 2 and Z-planes 3 and 4 were similar, although the central Z-planes (2,3) had slightly fewer monocular units. For $z_{pat} = 2.0$, all Z-planes were similar, although the position of the boundary between left and right eyes gradually moved in the same direction from one Z-plane to the next.

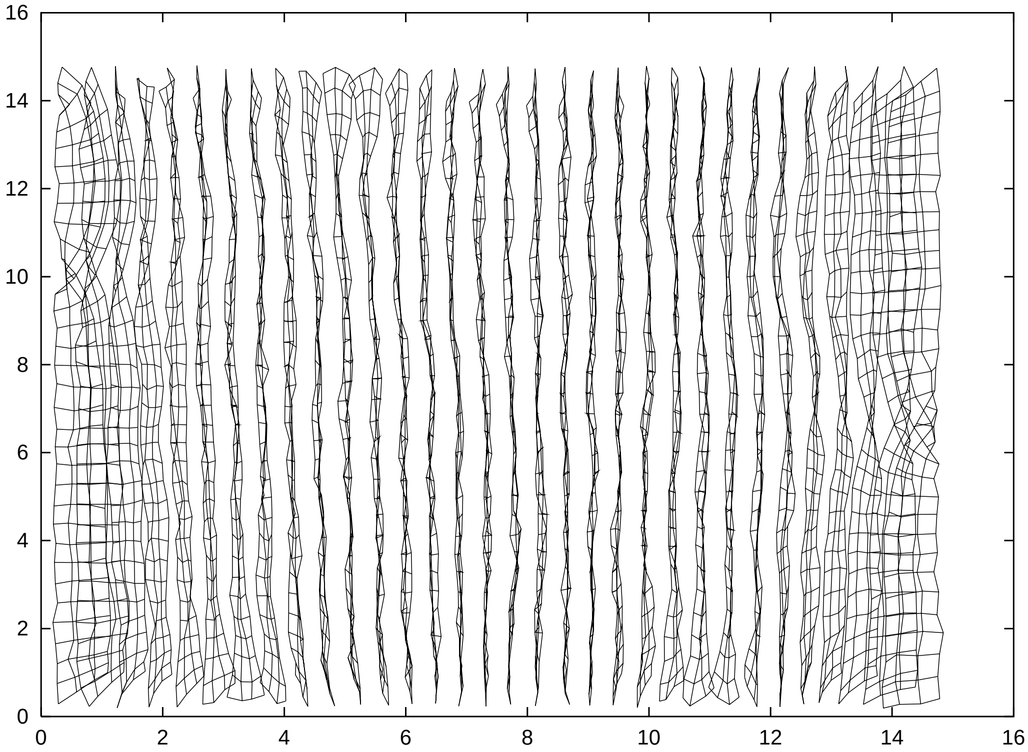

(a) All 32 X-planes

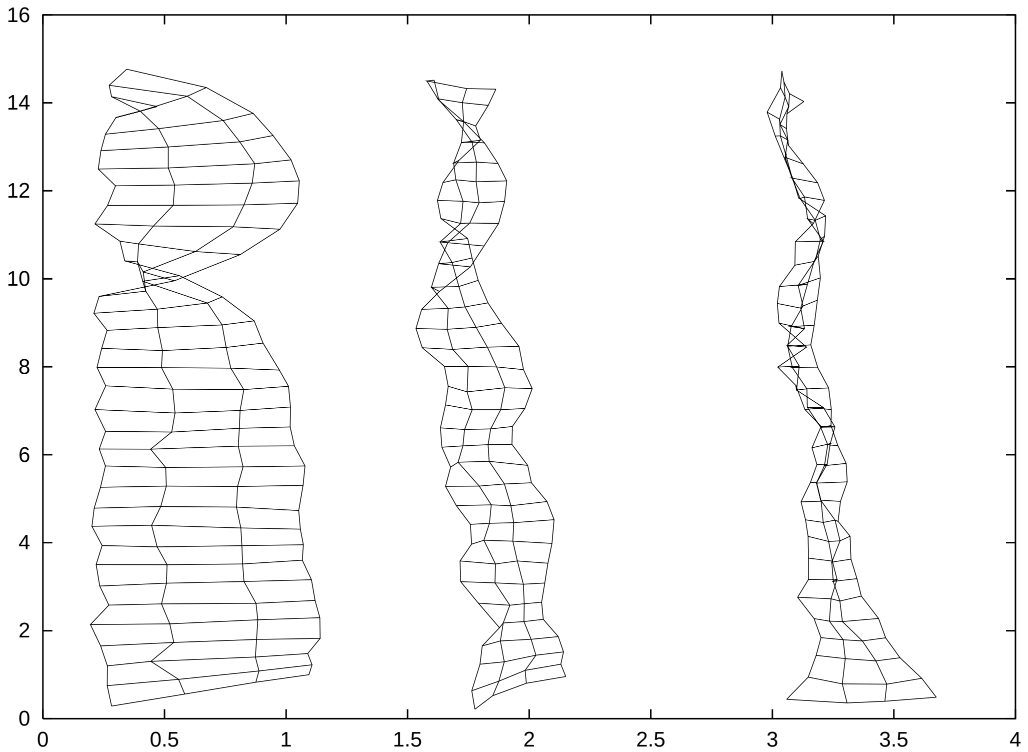

(b) X-planes 1,4 and 7

Figure 6.5: Final topography plots analysed in the X-planes for a three-dimensional network with $z_{pat} = 0.2$ and $Z_{\text{post}} = 4$. (a): The 32 topographic maps for each set of 32×4 units in the X-plane X$= i$, for all $i = 1 \ldots 32$. The map on the far left corresponds to X-plane X$= 1$, with the remaining maps following in order. (b): Three of the topographic maps in more detail, corresponding to (from left to right) X-planes 1,4 and 7. Each map on its own covers only a small region of the visual space, but together all of the maps completely cover the visual space.

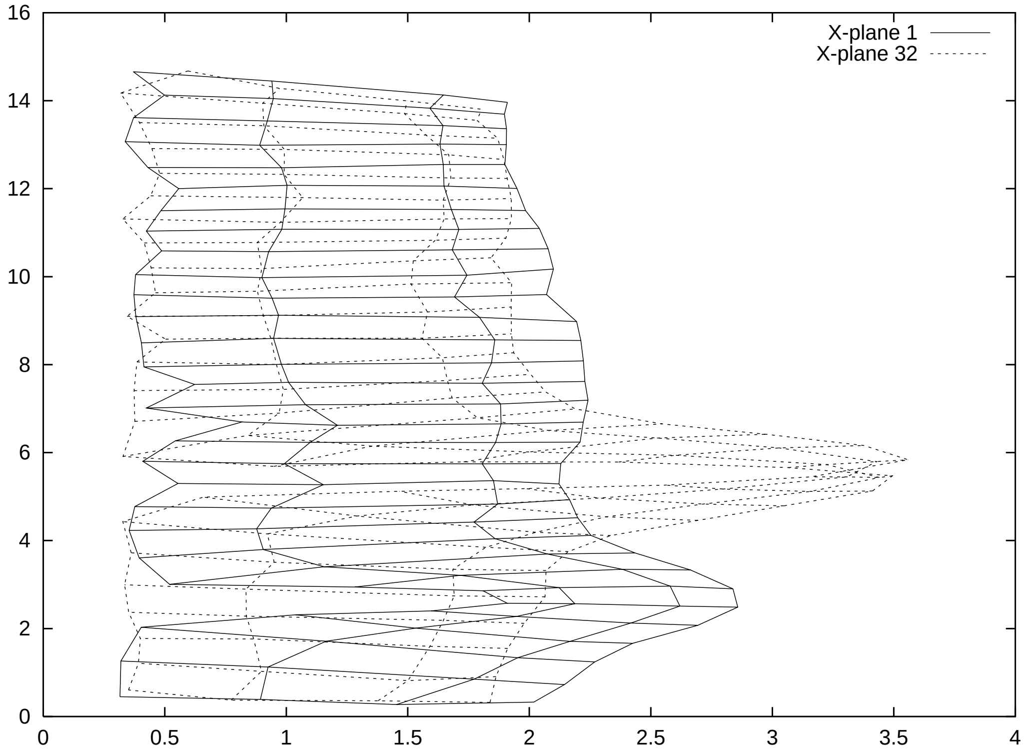

(a) X-planes 1 and 32

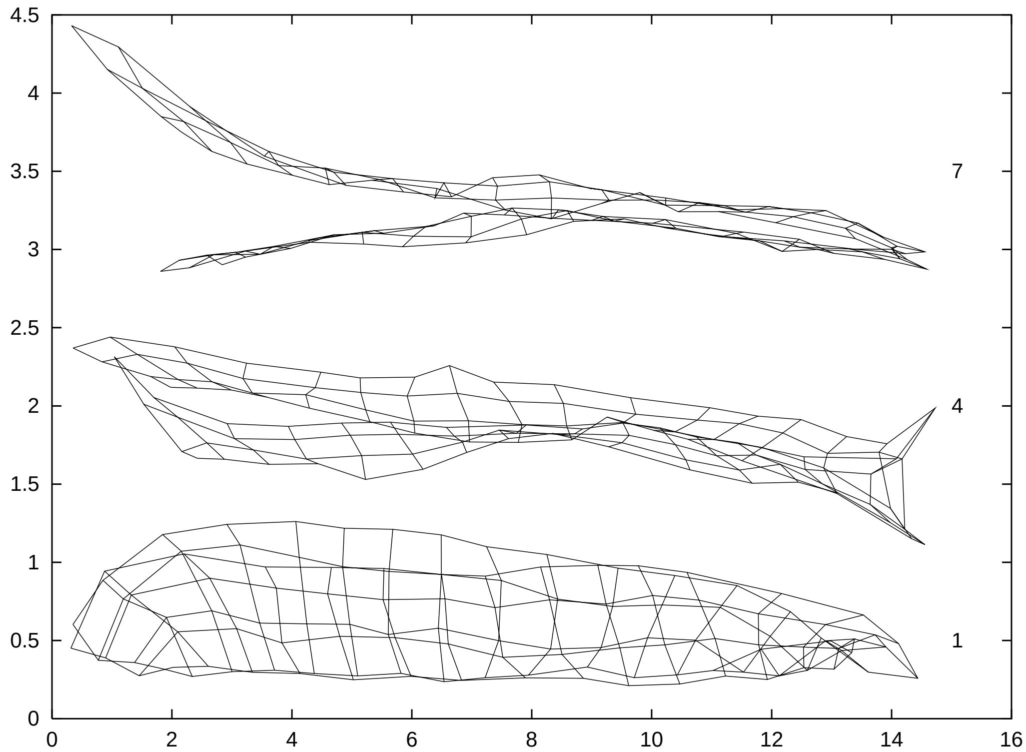

(b) Y-planes 1,4 and 7

Figure 6.6: Final topography plots analysed in X-planes and Y-planes for a three-dimensional network with $z_{pat} = 2.0$ and $Z_{\text{post}} = 4$. (a): The topographic maps for X-planes 1 and 32. These are the most medial (solid line) and lateral (dotted line) X-planes in the postsynaptic block. The two maps almost completely cover the same region of the input space. (b): The topographic maps for Y-planes 1, 4 and 7. Each map has folded over on top of itself to represent the same part of visual space twice. For each map, the fold has occurred in the region of visual space corresponding to $X \approx 14$.

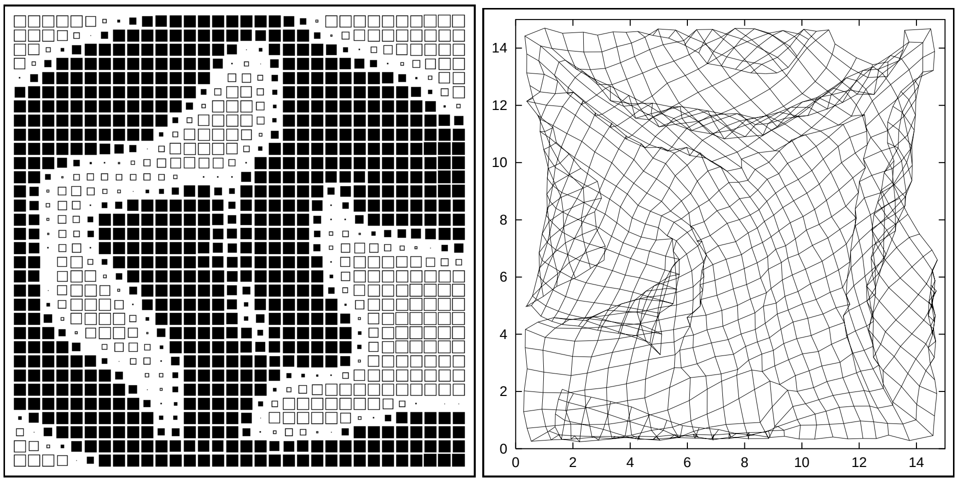

(a) $z_{pat} = 1.0$, Z-plane 1

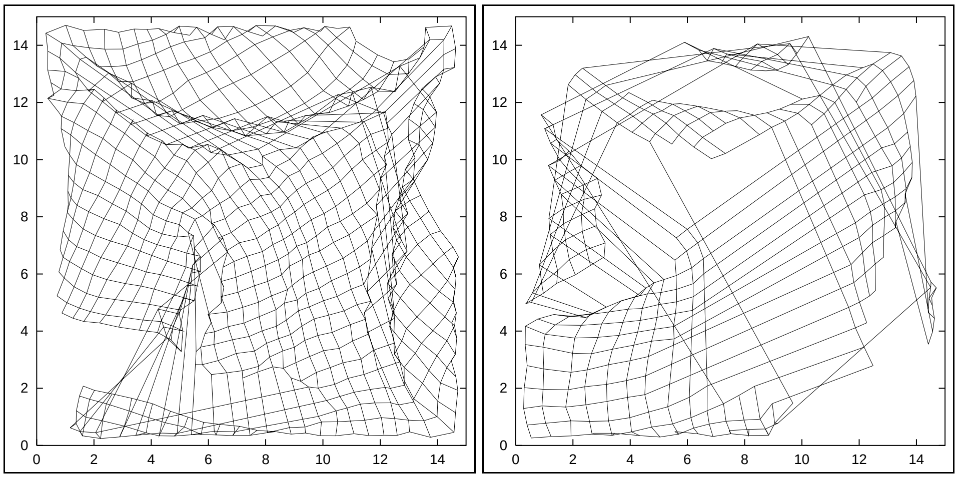

(b) Representation of visual space for each eye in Z-plane 1

Figure 6.7: Final topography and ocularity maps in a three-dimensional network with $z_{pat} = 1.0$ and $Z_{\text{post}} = 3$. (a): Topography and ocularity plots for Z-plane 1. (b): Topography plots for Z-plane 1, separated for each eye (left: $z < 0$, right: $z > 0$.). At first sight, the topography plot in (a) looks similar to a normal convoluted map when ocularity is present as a secondary feature. Separating the topographic plot according to the ocularity of the postsynaptic unit shows however that the units responsive to each eye represent different parts of visual space.

6.6 Discussion

In this chapter, we have presented three main arguments for the development of ocular dominance stripes. Although these arguments were developed with segregation into ocular stripes in mind, two of them have some connection with ocular segregation in the LGN. In relation to the Keesing model, the first argument, the range of lateral interactions, does not apply since the model does not use lateral connectivity. The model does use a growth rule, but this is only used periodically during development, is excitatory only, and is activity-independent.

The second argument presented for stripe development, the competition between topography and ocularity, is relevant to retinogeniculate development. This argument suggests that stripes form when same-position units and same-eye units compete for the same region of postsynaptic space. The force driving this competition is the strength of the correlation between the presynaptic units. In the case of retinogeniculate development, retinal waves produce no between-eye correlations, and so we would expect same-eye units to cluster together rather than same-position units. In the absence of any bias in the initial weights, it is therefore expected that same-eye units should cluster together. However, as seen in the first set of retinogeniculate simulations (in Figure 4.4 on page 65), the postsynaptic sheet does not divide into two eye-specific regions unless there is some form of initial weight bias to help segregation.

The initial weight bias used in Chapter 4 is justified by the evidence that contralateral axons arrive at the LGN a few days earlier than ipsilateral axons (Shatz, 1983). However, the simulations presented here in Section 6.3.3 show that it is possible for ocularity maps to segregate into two eye-specific regions without any form of initial weight bias. This is probably because the Obermayer model uses the Kohonen rule for weight updates, and this rule adapts the weights of a group of neighbouring postsynaptic units at the same time. In contrast, the Keesing model has weaker interactions between neighbouring postsynaptic units, making global reorganisation of topography and ocularity more difficult.

The third argument for ocular dominance stripe formation is also relevant to the issue of retinogeniculate development. Ocular dominance stripes can form in networks when the dimensionality of features in the input space is larger than the dimensionality of the output space. In the case of cortical development of topography and ocularity, the input space has three features and the output space is only two-dimensional. As long as the variance of the ocularity feature is above a critical value, ocular dominance stripes form. In this chapter, ocularity variance is assumed to increase as the input stimuli become more monocular. In Section 6.3.3 we have replicated the results from (Obermayer et al., 1991) which show that as the ocularity variance increases, stripe width increases. For sufficiently high values of ocularity variance, ocular dominance stripes within a two-dimensional postsynaptic sheet coalesce into two eye-specific regions.

When the Obermayer model is extended so that postsynaptic units are arranged into a three-dimensional block, ocularity stripes are no longer present, as shown in Section 6.4. In this case, the three input features can independently map onto the three dimensions of the postsynaptic block, although the relative variance of each of the features still controls the layout of the map. When the variance of the ocularity feature is small in comparison with the centre of mass features ($z_{pat} = 0.2$), ocularity maps onto the smallest dimension of the postsynaptic block (Z). The other features representing centre of mass are mapped onto the X and Y dimensions of the postsynaptic block. So, even when the network does not need to perform dimension reduction, the variance of each feature controls how they map into the postsynaptic block.

As the variance of ocularity is increased ($z_{pat} = 2.0$), ocularity maps onto the X dimension of the postsynaptic block, one of the two big dimensions. The centre of mass features are then forced to map onto the remaining dimensions of the postsynaptic block. However, because the value of z for each postsynaptic unit is always $\pm z_{pat}$, the x centre of mass value can also map onto the X dimension of the postsynaptic block, rather than the Z dimension which has eight times fewer units (32 versus 4). In this case, the Z dimension is ignored. Hence, we find that most units (excluding those on the boundary between left and right eye regions) at the same (X,Y) position but at different depths respond to the same eye and the same region of visual space.

In the case of retinal waves driving retinogeniculate development, since the between-eye correlations are very small, the corresponding variance of ocularity should also be quite small (favouring $z_{pat} = 0.2$ rather than $z_{pat} = 2.0$). The Obermayer model therefore predicts that the ocularity feature maps onto the dorso-ventral dimension of the LGN because this is the smallest dimension of the LGN and ocularity is the feature with the smallest variance. In principle this means that the retinal axons could self-organise into eye-specific layers given completely random initial conditions. However, in practice this probably does not happen because of the limited retinal axonal branching. Furthermore, there is no real need for global reorganisation to occur if other mechanisms, such as the earlier arrival of contralateral axons, already impose a global map layout.